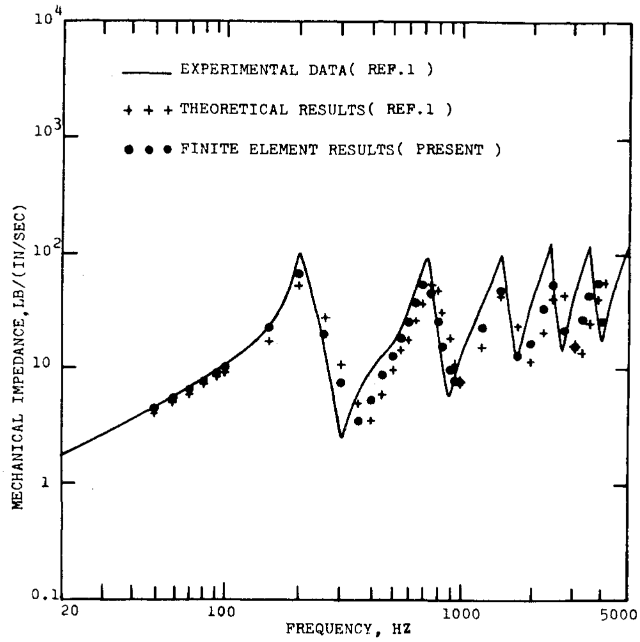

Fig. 2 Mechanical point impedance of the three layer sandwich ring under concentrated periodical loading.

The multilayer hybrid stress flat plate element has been well documented in Refs. 3 and 4. It suffices to say that the element boundary displacements are linear, that each layer has independent rotations, and that transverse shear deformation and rotatory inertia are included. The mass matrix is a nondiagonal hybrid-rational one.[5] The modelling of curved surfaces by the flat plate element has been tested and found to be satisfactory.[4]

The problem considered here is the second ring problem of Ref. 1. Numbering from the outermost layer to the innermost layer, the following data are used in the calculation: thickness (in.) $h_1 = 0.0747$, $h_2 = 0.004$, $h_3 = 0.25$; density (lb-in.^{4}/sec^2) $\gamma_1 = \gamma_3 = 0.725 \times 10^{-3}$, $\gamma_2 = 0.103 \times 10^{-3}$; Young's modulus (psi) $E_1 = E_3 = 30 \times 10^6$; Poisson's ratio $v_1 = v_3 = 0.3$. The radius to the middle surface of the first layer $R_1 = 4.3538$ in. and the width of the ring $b = 2$ in. The viscous central core is characterized by its frequency and temperature dependent complex shear modulus

$$G_2 = (1+1.46i)\exp[0.494\ln(\omega/2\pi)+3.022] \tag{5}$$

at 72°F. In the finite element computation, the Poisson's ratio v_2 for this layer is assumed to be 0.3 and its Young's modulus E_2 is determined from G_2 and v_2.

The ring is freely supported undergoing a concentrated radial force $P_0 e^{i\omega t}$ acting on top of the first layer. Because of symmetry, only half of the ring is modelled by one row of 36 identical elements in the circumferential direction. The load P_0 is equally divided and applied to the top two nodes of the first element.

Table 1 Comparison of double and single precision solutions

Frequency, Hz ($\omega/2\pi$)	Impedance, lb/(in./sec) Double precision	Single precision
50	4.192	8.038
100	9.883	14.317
350	3.435	3.423
600	24.657	24.850
850	15.850	15.800
1500	47.914	47.886
2750	19.695	19.684
4000	25.795	25.785

The resulting mechanical impedance at the loading point is plotted in Fig. 2 against the analytical and experimental results reported in Ref. 1. It is seen that the present finite element solution is very accurate. The slightly better result over the analytical solution of Ref. 1 may be attributed to the fact that the present finite element modeling allows independent rotations for each layer and rotatory inertia is included.

For low frequency responses, some precaution must be taken to avoid getting erroneous results. The elements of the **K** matrix of this problem are in the order of 10^8 and the elements of the **M** matrix are in the order of 10^{-4}. For small ω, the effect of **M** matrix may be wiped out due to the round off of the computer and the essential rigid body response may be distorted. Such errors can be avoided simply by using double precision calculation. The effect of this can be seen in Table 1, where both double precision and single precision solutions, obtained on an IBM 370/M165, are listed for eight selected values of ω. The double precision solutions are those used in plotting Fig. 2. For $\omega/2\pi$ smaller than 350 Hz, the single precision solutions are erroneous.

References

[1] Lu, Y. P., Douglas, B. E., and Thomas, E. V., "Mechanical Impedance of Damped Three-Layered Sandwich Rings," *AIAA Journal*, Vol. 11, No. 3, March 1973, pp. 300–304.

[2] Abel, J. F., "Static and Dynamic Analysis of Sandwich Shells with Viscoelastic Damping," SESM 68-9, Aug. 1968, Structural Engineering Lab., Univ. of California, Berkeley, Calif.

[3] Mau, S. T., Tong, P., and Pian, T. H. H., "Finite Element Solutions for Laminated Thick Plates," *Journal of Composite Materials*, Vol. 6, April 1972, pp. 304–311.

[4] Mau, S. T., Pian, T. H. H., and Tong, P., "Vibrational Analysis of Laminated Plates and Shells by a Hybrid Stress Element," *AIAA Journal*, Vol. 11, No. 10, Oct. 1973, pp. 1450–1452.

[5] Tong, P., Mau, S. T., and Pian, T. H. H., "Derivation of Geometric Stiffness and Mass Matrices for Finite Element Hybrid Models," submitted to the *International Journal of Solids and Structures*.

Biot's Variational Principle for Aerodynamic Ablation of Melting Solids

ANANT PRASAD*
Birla Institute of Technology and Science, Pilani, India

AND

H. C. AGRAWAL†
Indian Institute of Technology, Kanpur, India

Nomenclature

c = heat capacity per unit volume of the material
h = heat-transfer coefficient
H = heat flow vector
k = conductivity of the material
L = latent heat of the material
$q_1(t)$ = unknown surface temperature
$q_2(t)$ = melting distance
t = time

Received August 9, 1973.
Index categories: Heat Conduction; Material Ablation.

* Lecturer, Department of Mechanical Engineering; presently, research student, Department of Mechanical Engineering, University of Liverpool, Liverpool, England.

† Associate Professor, Department of Mechanical Engineering; presently, Senior Technologist, Research & Development Laboratories, Pilkington Brothers Ltd, Lathom, Ormskirk (Lancashire), England (on leave of absence).

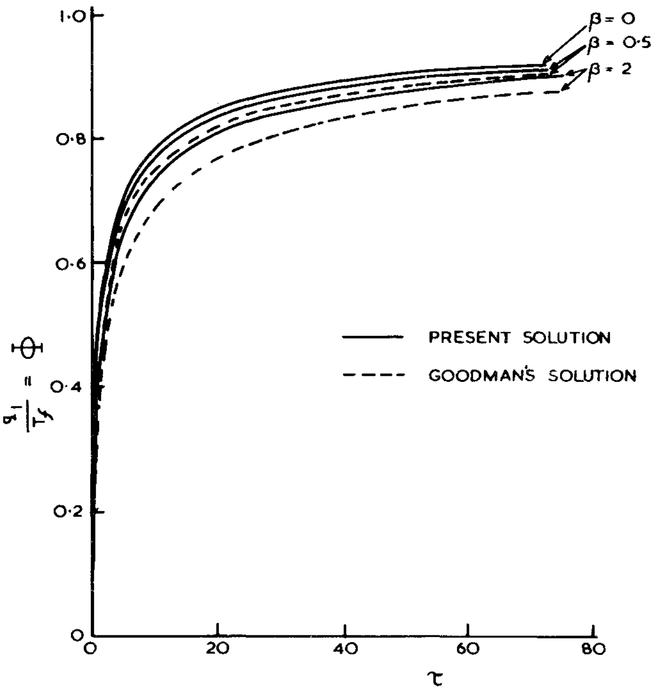

Fig. 1 Nondimensional surface temperature–time history.

T_f = temperature of the surroundings
α = thermal diffusivity
β = dimensionless temperature of the surroundings, $cT_f/\rho L$
η = dimensionless melting distance, hq_2/k
θ = temperature distribution in the melt
ρ = density of the material
τ = dimensionless time, $(h^2 T_f t)/\rho Lk$
Φ = dimensionless surface temperature, q_1/T_f

Introduction

BIOT'S variational principle has been successfully applied for solving the phase-change problem with different boundary conditions, by workers[1–4] in the past. In an earlier paper,[5] the present authors had used this approach to the phase-change problem with constant heat flux as the boundary condition and without removal of melt. The purpose of the present Note is to extend the applicability of Biot's method to aerodynamic ablation of melting bodies, i.e., when the heat flux at the boundary is generated aerodynamically.

Formulation of the Problem

One-dimensional heating of a semi-infinite solid of constant thermal properties is considered. After initiation of melting, let T_f and $q_1(0, t)$ be the temperature of the surrounding medium and the surface temperature of the melt, respectively, and h, the heat-transfer coefficient. The distance of the melt line from the surface after time t is denoted by $q_2(t)$. Time t is measured from the initiation of melting. The problem is simplified by assuming all the solid to be at the melting temperature, although there is a temperature distribution in the solid as well. The validity of this assumption is discussed by Goodman.[6] The equation describing the process is

$$\partial^2\theta/\partial x^2 = (1/\alpha)\partial\theta/\partial t, \quad x > 0, \quad t > 0 \tag{1}$$

Initial and boundary conditions are

$$\theta = 0, \qquad t = 0 \tag{2}$$

$$q_2(t) = 0, \qquad t = 0 \tag{3}$$

$$-k\,\partial\theta/\partial x = h(T_f - q_1), \quad x = 0, \ t > 0, \ T_f > q_1 \tag{4}$$

The assumption of constant temperature in the solid reduces the boundary condition at the interface to

$$\dot{H} = L\dot{q}_2, \quad x = q_2(t), \quad t > 0 \tag{5}$$

where $\dot{H}$ denotes the heat-flow rate and $H = Lq_2$. The melting temperature is taken to be zero.

Solution

A linear temperature distribution in the melt is assumed as

$$\theta = q_1(1 - x/q_2) \tag{6}$$

where q_1 and q_2 are generalized coordinates representing the surface temperature and the melting distance, respectively, to be determined. The energy conservation is given by

$$\operatorname{div} H = -c\theta \tag{7}$$

Equation (6) together with Eq. (7), gives the heat flowfield

$$H = (\tfrac{1}{2})cq_1 q_2(1 - x/q_2)^2 + \rho L q_2 \tag{8}$$

which satisfies the boundary condition, Eq. (5). The expressions for the temperature distribution, Eq. (6), and the heat flowfield, Eq. (8), being known, Biot's variational principle can be easily applied which leads to the Lagrangian equation

$$\partial V/\partial q_2 + \partial D/\partial \dot{q}_2 = Q_2 \tag{9}$$

The function V represents the thermal potential, D, the dissipation function, and Q_2, the thermal force and they are given by

$$V = (\tfrac{1}{2})\int_0^{q_2} c\theta^2\,dx \tag{10}$$

$$D = (1/2k)\int_0^{q_2} \dot{H}^2\,dx \tag{11}$$

Fig. 2 Nondimensional melting-time history.

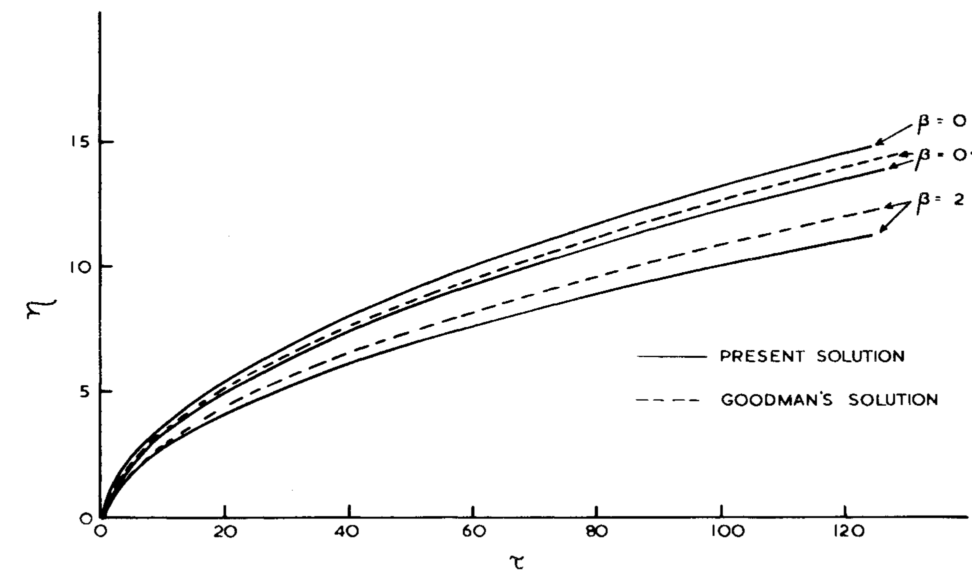

$$Q_2 = (\theta)_{x=0}(\partial H/\partial q_2)_{x=0} \quad (12)$$

Using Eqs. (6) and (10), we get

$$V = (\tfrac{1}{6})cq_1^2 q_2 \quad (13)$$

$$\partial V/\partial q_2 = (\tfrac{1}{6})cq_1^2 \quad (14)$$

The time rate of change of heat flow obtained from Eq. (8), is

$$\dot{H} = (\tfrac{1}{2})c(q_1\dot{q}_2 + \dot{q}_1 q_2)(1-x/q_2)^2 + cq_1\dot{q}_2(x/q_2)(1-x/q_2) + \rho L\dot{q}_2 \quad (15)$$

and

$$\partial H/\partial q_2 = (\tfrac{1}{2})cq_1(1-x/q_2)^2 + cq_1(x/q_2)(1-x/q_2) + \rho L \quad (16)$$

Substituting Eq. (15) in Eq. (11) and Eq. (16) in Eq. (12), it gives

$$D = (1/2k)[(c^2 q_2/20)(q_1\dot{q}_2 + \dot{q}_1 q_2)^2 + (c^2 q_1^2 q_2 \dot{q}_2^2/30) + \rho^2 L^2 q_2 \dot{q}_2^2 + (q_1\dot{q}_2 + \dot{q}_1 q_2)(c^2 q_1 q_2 \dot{q}_2/20 + c\rho L q_2 \dot{q}_2/3) + c\rho L q_1 q_2 \dot{q}_2^2/3] \quad (17)$$

$$\partial D/\partial \dot{q}_2 = (q_2\dot{q}_2/2k)(2\rho^2 L^2 + 4c\rho L q_1/3 + 4c^2 q_1^2/15) + (q_2^2 \dot{q}_1/2k)(3c^2 q_1/20 + c\rho L/3) \quad (18)$$

and

$$Q_2 = (cq_1^2/2) + \rho L q_1 \quad (19)$$

The Lagrangian equation, Eq. (9), in the generalized coordinate q_2, becomes

$$(q_2\dot{q}_2/2k)(2\rho^2 L^2 + 4c\rho L q_1/3 + 4c^2 q_1^2/15) + (q_2^2\dot{q}_1/2k)(3c^2 q_1/20 + c\rho L/3) = cq_1^2/3 + \rho L q_1 \quad (20)$$

Using Eq. (6), the boundary condition, Eq. (4), is given by

$$h(T_f - q_1) - k(q_1/q_2) = 0 \quad (21)$$

Use of this boundary condition, Eq. (21), at the surface, provides an additional relation between the generalized coordinates and thus reduces by one the number of differential equations of the Lagrangian type. We now nondimensionalize Eqs. (20) and (21) by defining the following quantities

$$\tau = h^2 T_f t/\rho L k$$
$$\eta = hq_2/k$$
$$\beta = cT_f/\rho L$$
$$\Phi = q_1/T_f$$

Equation (21), in the dimensionless form, gives the surface temperature

$$q_1/T_f = \Phi = \eta/(1+\eta) \quad (22)$$

Equation (20), in the dimensionless form, after simplification, becomes

$$\dot{\eta}[A_1\eta^3 + A_2\eta^2 + A_3\eta + A_4] = B_1\eta^2 + B_2\eta + B_3 \quad (23)$$

where

$$A_1 = 16\beta^2 + 80\beta + 120 \qquad B_1 = 40(\beta+3)$$
$$A_2 = 25\beta^2 + 180\beta + 360 \qquad B_2 = 40(\beta+6)$$
$$A_3 = 100\beta + 360 \qquad B_3 = 120$$
$$A_4 = 120$$

Solution of Eq. (23) gives the melting rate

$$\tau = (A_1/2B_1)\eta^2 + (A_2 - A_1 B_2/B_1)(\eta/B_1) + [(1/2B_1)(A_3 - A_1 B_3/B_1) - (B_2/2B_1)(A_2 - A_1 B_2/B_1)] \times [\ln(B_1\eta^2 + B_2\eta + B_3)/B_3] + [A_4 + (A_2 - A_1 B_2/B_1) \times (B_2^2 - 2B_1 B_3)/2B_1^2 - (B_2/2B_1)(A_3 - A_1 B_3/B_1)] \times (2/(4B_1 B_3 - B_2^2)^{1/2}) \times [\tan^{-1}(2B_1\eta + B_2)/(4B_1 B_3 - B_2^2)^{1/2} - \tan^{-1}(B_2)/(4B_1 B_3 - B_2^2)] \quad (24)$$

It can be easily seen that for very high latent heat ($L \to \infty$, $\beta \to 0$), Eq. (24) reduces to

$$\tau = (\eta^2/2) + \eta \quad (25)$$

This is the same equation as obtained by Goodman,[6] for the melting rate, using the heat balance integral method. Results for surface temperature–time history $\Phi(\tau)$ and the melting rate $\eta(\tau)$ for different values of β are plotted in Figs. 1 and 2, respectively, and compared with Goodman's solution.

It is concluded that Biot's variational method is applicable to the phase-change problem with aerodynamic heating. The simplicity of the method lies in using only a linear temperature profile, yielding satisfactory results.

References

[1] Lardner, T. J., "Approximate Solutions to Phase-Change Problems," *AIAA Journal*, Vol. 5, No. 11, Nov. 1967, pp. 2079–2080.

[2] Biot, M. A. and Daughaday, H., "Variational Analysis of Ablation," *Journal of the Aerospace Sciences*, Vol. 29, No. 2, Feb. 1962, pp. 227–229.

[3] Biot, M. A. and Agrawal, H. C., "Variational Analysis of Ablation for Variable Properties," *Transactions of the ASME, Ser. C: Journal of Heat Transfer*, Vol. 86, No. 3, Aug. 1964, pp. 437–442.

[4] Prasad, A., "Biot's Variational Principle in a Phase-Change Problem," Master's thesis, Oct. 1968, Dept. of Mechanical Engineering, Indian Institute of Technology, Kanpur, India.

[5] Prasad, A. and Agrawal, H. C., "Biot's Variational Principle for a Stefan Problem," *AIAA Journal*, Vol. 10, No. 3, March 1972, pp. 325–327.

[6] Goodman, T. R., "The Heat-Balance Integral and Its Application to Problems Involving a Change of Phase," *Transactions of the ASME*, Vol. 80, No. 3, Feb. 1958, pp. 335–342.

Compressibility Effects in Unsteady Thin-Airfoil Theory

Roy K. Amiet*

United Aircraft Research Laboratories, East Hartford, Conn.

Nomenclature

- b = semichord
- $C(k)$ = Theodorsen function
- $f(M)$ = function of Mach number, defined by Eq. (8b)
- g = kernel function defined by Eq. (7b)
- h = kernel function defined by Eq. (8b) or Eq. (10)
- J_n = Bessel function
- k = reduced frequency, $\omega b/U$
- k^* = k/β^2
- L = lift
- M = Mach number
- $\mathcal{M}$ = moment about midchord
- P = pressure
- $S(k)$ = Sears function
- t = time
- U = freestream velocity
- w = upwash
- x = axial coordinate
- y = coordinate normal to freestream
- β = $(1-M^2)^{1/2}$
- γ = Euler's constant
- ε = Mk
- θ = $-\cos^{-1} x$
- ρ = freestream density
- φ = $-\cos^{-1} x_1$
- ϕ = velocity potential

Received August 23, 1973; revision received October 4, 1973. This work was supported by the Pratt and Whitney Aircraft Division, Acoustics Group, under Engineering Order Supplement 730050-526.

Index categories: Nonsteady Aerodynamics; Subsonic and Transonic Flow.

* Research Engineer.